



"Gheorghe Asachi" Technical University of Iasi, Romania



POTENTIAL USE OF *Crambe abyssinica* PRESS CAKE AS AN ADSORBENT: BATCH AND CONTINUOUS STUDIES

Adriana S. Franca^{1*}, Leandro S. Oliveira¹, Victor F. Oliveira², Cibele C.O. Alves¹¹DEMEC/UFMG, Universidade Federal de Minas Gerais, Av. Antônio Carlos 6627, 31270-901 Belo Horizonte, MG Brazil²DEQ/UFMG, Universidade Federal de Minas Gerais, Av. Antônio Carlos 6627, 31270-901 Belo Horizonte, MG Brazil

Abstract

This study evaluates the potential of *Crambe abyssinica* press cake, a residue from crambe oil extraction and/or biodiesel production, as an adsorbent for removal of cationic dyes from wastewaters. Batch adsorption tests were performed at 30, 40 and 50°C. Adsorption kinetics and equilibrium were satisfactorily described by the pseudo second-order and Freundlich models, respectively. Adsorption was spontaneous and exothermic. Fixed bed adsorption (breakthrough curve) was satisfactorily described by the Dose-Response model. The obtained values of maximum adsorption capacity were 79.7 and 102.5 mg g⁻¹ in batch and continuous systems, respectively. Adsorption tests showed that crambe press cake, without any thermal treatment, presented higher adsorption capacity than activated carbons produced from other oilseed press cakes (sunflower, coffee and *Raphanus sativus*), confirming that this type of waste material is a suitable candidate for use in the production of adsorbents.

Key words: adsorption, biodiesel solid waste, cationic dyes, crambe

Received: March, 2012; Revised final: October, 2012; Accepted: November, 2012

1. Introduction

Crambe abyssinica is a cruciferous oilseed plant (classified under the genus *Crambe* and the family Cruciferae) that presents fast growth, tolerance to either low or high temperatures, low nutrient requirements and low cultivation costs (Wang et al., 2000). Interest in this specific crop is usually associated to its high oil content (32 – 36%) and also the high erucic acid content of the oil (55–60%). Crambe oil and derivatives present a wide variety of applications including lubricants, hydraulic, dielectric and refrigerating fluids, biodiesel, rubber additives, polymers, base for paints and coatings, waxes, and others (Falasca et al., 2010; Wang et al., 2000).

Crambe meal presents good quality protein, but its use as livestock feed is restricted due to high contents of glucosinolates and tannins (Wang et al., 2000). One of the effective uses of agricultural waste biomass that has gained attention over the last decade

is the production of low-cost adsorbents for wastewater treatment, with applications in the removal of organic pollutants, heavy metals and dyes (Ali et al., 2012; Bhatnagar and Sillanpää, 2010; Bulgariu et al., 2007; Guerrero-Coronilla et al., 2014; Lopez-Núñez et al., 2014) with some recent reports focusing on the use of inedible seed press cakes as raw materials for the production of adsorbents. Examples include oil palm fiber (Tan et al., 2007), sunflower oil cake (Karagöz et al., 2008), defective coffee beans press cake (Franca et al., 2010; Nunes et al., 2009) and *Raphanus sativus* press cake (Lázaro et al., 2008; Nunes et al., 2011). The produced adsorbents were successfully employed for dye adsorption (methylene blue and malachite green). Furthermore, recent studies have also verified the feasibility of employing inedible seed press cakes directly as adsorbents, i.e., production of adsorbents with minimum treatment (excess oil removal, drying and grinding) and without submitting the agricultural waste to any thermal and/or chemical activation

* Author to whom all correspondence should be addressed: e-mail: adriana@demec.ufmg.br; Phone: +55-31-34093512; Fax: +55-31-34433783

procedure. Reported applications include adsorption of copper by mustard oil seed cake (Ajmal et al., 2005), adsorption of pesticides in cold-pressed rapeseed, moringa, mustard and soybean cakes (Boucher et al., 2007), removal of cadmium and chromium by *Jatropha* oil cake (Garg et al., 2007, 2008) and adsorption of methylene blue by *Madhuca indica* seeds (Gottipati and Mishra, 2010).

In view of the aforementioned, and considering that there is no literature available on the use of *Crambe abyssinica* press cake as an adsorbent, the objective of the present study was to evaluate the performance of such agricultural waste as a low-cost adsorbent for wastewater treatment. Methylene blue ($C_{16}H_{18}N_3S$) was selected as a model adsorbate in order to allow for performance comparison with respect to other seed press cakes that have been previously employed as adsorbents. Given that adsorption processes for purification of wastewaters can be carried out either discontinuously, in batch reactors, or continuously, in fixed-bed columns, the performance of the adsorbent was evaluated in both batch and column tests.

2. Experimental

2.1. Materials

Crambe abyssinica seeds were screw-pressed (Ecirtec, Brazil) for oil removal. Excess oil removal was performed by hexane extraction at 60°C for 1h. The cationic dye used as target adsorbate was methylene blue (MB - C.I. 52015), 15% hydrated, 95% purity, purchased from Labsynth Lab Products (São Paulo, Brazil). MB stock solutions (1000 mg/L) were prepared in distilled water. Working solutions (50 to 700 mg/L) were prepared by diluting the stock solution with distilled water prior to each adsorption test.

2.2. Adsorbent characterization

Evaluation of the Point of Zero Charge (pH_{PZC}) was based on a mass titration procedure (Noh and Schwarz, 1990). Three aqueous solutions of different pH's (3,6 and 11) were prepared. Several amounts of the adsorbent (0.05%, 0.1%, 0.5%, 1.0%, 3.0%, 7.0% and 10.0% w/w) were added to 20 mL of each solution. The aqueous suspensions were then allowed to equilibrate for 24 h under agitation (100 rpm) at 25°C. The pH of each solution was measured using a digital pHmeter (Micronal, São Paulo, Brazil) and the pH_{PZC} was determined as the converging pH value from the pH vs. adsorbent mass curve. Surface functional groups determination was based on the Boehm titration method (Boehm, 1994). Solutions of $NaHCO_3$ (0.1 mol L^{-1}), Na_2CO_3 (0.05 mol L^{-1}), $NaOH$ (0.1 mol L^{-1}), and HCl (0.1 mol L^{-1}) were prepared with distilled water. 50 mL of each solution were added to vials containing 1 g of the adsorbent, shaken for 24h (100 rpm) and then filtered. Five solution blanks were also prepared. The excess of

base or acid was then determined by back titration with $NaOH$ (0.1 mol L^{-1}) and HCl (0.1 mol L^{-1}) solutions. The amounts of the different oxygenated acidic surface groups (carboxylic, phenolic and lactonic) were evaluated according to the difference in the calculated amount of surface functionality reacted with the specified bases. $NaOH$ reacts with all surface groups, (carboxylic, lactonic, and phenolic), and will therefore present a calculated amount of surface functionality reacted that includes all of these groups. Na_2CO_3 reacts with carboxylic and lactonic groups and the difference between the amount of surface functionality reacted measured with $NaOH$ and that measured with Na_2CO_3 will denote the number of phenolic groups on the surface. Similarly, since $NaHCO_3$ reacts only with carboxylic groups, the difference between the amount of surface functionality reacted with Na_2CO_3 and with $NaHCO_3$ represents the number of lactonic groups. The amount of carboxylic groups was found directly from the titration with $NaHCO_3$. The surface structure of the adsorbent was evaluated by Fourier Transform Infrared (FTIR) spectroscopy. The corresponding spectra were obtained on a Series 102 ABB BOMEM FTIR spectrometer (Quebec, Canada). The equipment was operated in the wavenumber range of 400–4000 cm^{-1} , with a resolution of 4 cm^{-1} .

2.3. Batch adsorption studies

Batch adsorption experiments were performed employing 250 mL Erlenmeyer flasks. The flasks were agitated on an orbital shaker at 100 rpm for pre-determined time intervals. For each experiment, a pre-determined amount of adsorbent was thoroughly mixed with 100 mL of MB solution. Preliminary tests were conducted for the following fixed parameters: initial MB concentration = 200 mg L^{-1} , initial pH = 5 and adsorbent concentration = 10 g L^{-1} . Effect of particle size (diameter = D) was evaluated in the following particle diameter ranges: $D < 0.43$ mm; $0.43 < D < 0.84$ mm; $0.84 < D < 1.00$ mm; and $D > 1.00$ mm. Effects of pH and adsorbent concentration were studied in the respective ranges of 5 to 10 and of 5 to 30 g L^{-1} , at a fixed initial dye concentration (200 mg L^{-1}). Effect of contact time was evaluated at time periods ranging from 5 min to 8 hours and initial dye concentrations ranging from 50 to 700 mg L^{-1} at a fixed adsorbent dosage (10 g L^{-1}). All tests were executed in two replicates. After previously stipulated time sampling periods, 2 mL aliquots were taken from the Erlenmeyer flasks (maximum of 2 aliquots or 4mL per flask). Each sample was then centrifuged and the corresponding MB concentration was evaluated by a spectrophotometer (Cole Parmer 1100 RS) at 665 nm. The amount of MB adsorbed was calculated based on the difference between the initial MB concentration and the MB concentration in the solution at the specific sampling time. All measurements were performed in three replicates per experiment and the average values were reported.

2.4. Continuous adsorption studies

Continuous flow adsorption experiments were performed employing a cylindrical stainless steel column (10 cm height and 2.5 cm internal diameter). Known quantities of adsorbent (12.13 g) were placed into the column to yield the desired bed height (6 cm). MB solutions at of different initial concentrations (200, 500 and 700 mgL⁻¹) (pH 5.8) were pumped downward through the column bed. At different time intervals samples were collected at the column outlet and analyzed for MB concentration by a spectrophotometer (Cole Parmer 1100 RS) at 665 nm. Each experiment was conducted until the MB effluent concentration attained 99.5% of its inlet concentration. The flow rate was varied from 11.5 to 21.5 mL/min.

3. Results and discussion

3.1. Preliminary adsorption tests

Preliminary tests were conducted in order to verify the effect of temperature and pH on the stability of the adsorbent, i.e., to ascertain if, under the studied conditions, the solid would release any chemical substances that would distort absorbance readings and consequently MB dosage. Batch contact experiments were conducted for 6 h at 30, 40 and 50°C, employing distilled water, with the initial pH being adjusted to the following values: 3, 5, 7, 9 and 11. No significant variations in absorbance values were detected for the pH and temperatures evaluated, with an average deviation of 0.30±0.02 mg/L in concentration readings. Such values were considered to be within acceptable experimental deviation.

Batch adsorption tests (initial pH 5, initial MB concentration 200 mg g⁻¹, adsorbent dosage 10 g L⁻¹) were also performed in order to evaluate the effect of residual oil on adsorption efficiency. The removal of residual oil by hexane extraction provided an increase in adsorption efficiency from 73 to 79% after 6 h adsorption. Adsorbed amounts after 6 h were 13.2 and 14.1 mg g⁻¹ for the crambe press cake before and after residual oil extraction, respectively, without any thermal treatment. The corresponding values for other press cakes submitted to carbonization at 800°C were 10.5 mg g⁻¹ for *Raphanus sativus* press cake (Lázaro et al., 2008) and 9.2 mg g⁻¹ for defective coffee press cake (Nunes et al., 2009). Given that the crambe press cake, without thermal treatment, presented higher adsorption capacity in comparison to other thermally processed press cakes, the remaining adsorption tests were conducted with the crambe press cake submitted to 1 h hexane extraction for residual oil recovery (CPC).

3.2. Adsorbent characterization

Results for pHPZC determination indicated a pHPZC value of approximately 5.7, and therefore pH values should be maintained above this value to

ensure a predominant negatively charged surface and favor adsorption by electrostatic attraction of the MB cation. However, given the possibility of MB dimerization and/or reaction with NaOH at high pH values (Nunes et al., 2009), the maximum initial solution pH value employed in the present study was 10. The functional groups at the surface of adsorbent, characterized by the Boehm method, were predominantly acid (0.70 ± 0.04 mmol/g adsorbent), distributed as follows: carboxylic (0.38 ± 0.03 mmol/g adsorbent), phenolic (0.18 ± 0.04 mmol/g adsorbent) and lactonic (0.14 ± 0.03 mmol/g adsorbent). The concentration of basic groups was 0.42 ± 0.01 mmol/g adsorbent. The predominance of acid groups on the adsorbent surface is expected, given that no thermal treatment was applied. Other studies employing pressed seed cakes (Franca et al., 2010; Nunes et al., 2011) showed that even mild carbonization conditions will result on a decrease in the amount of carboxylic surface groups and consequent increase in pHPZC.

The FTIR spectra of CPC is shown in Fig. 1a. The absorption bands at 600-580 cm⁻¹ can be associated to bending modes of aromatic compounds (Garg et al., 2007). The band at 1058 cm⁻¹ can be assigned to the C-O group in carboxylic and alcoholic groups. Bands associated with the C=C stretching in aromatic rings were verified in the range 1625-1400 cm⁻¹. The identification of such groups has been reported regarding FTIR spectra obtained for *Jatropha* oil cake (Garg et al., 2007), in association to the presence of lignin. The band at 1462 cm⁻¹ is attributed to OH bending vibrations in association with phenolic groups (Garg et al., 2007). The band at 1650 cm⁻¹ is attributed to the presence of highly conjugated C=O groups such as carbonyl groups near hydroxyl ones. Two sharp bands were observed at 2865 and 2924 cm⁻¹, attributed to aliphatic C-H stretching vibration from cellulose and hemicellulose CH₂ groups (Hameed and Ahmad, 2009). The broad band with maximum at 3285 cm⁻¹ is associated to -OH groups, both free and bonded, being reported in most FTIR analyses of adsorbents (Garg et al., 2007; Nunes et al., 2009).

FTIR spectroscopy is also a fast and reliable analytical technique for the study of the types of interaction that might occur between an adsorbate and the surface of an adsorbent. Thus, this technique was herein used to provide an insight into the mechanisms of methylene blue adsorption onto crambe seed press-cake. The FTIR spectra for the hydrated solid dye (a), the press-cake (CPC) (b), and the methylene blue-loaded press-cake (c) are compared in Fig. 1. The hydrated solid dye was used to obtain the spectra for methylene blue since in aqueous solutions self association of the dye molecules will occur.

This self-association effect in the solution will reflect on the IR spectrum making it difficult to correlate with the spectrum characteristics of the adsorbed dye, which, in turn, are expected to be more closely related to the spectra of the condensed solid

state of the dye at higher adsorption capacities (Ovchinnikov et al., 2007). The FTIR spectrum for the crambe press-cake is typical of agricultural materials and the bands in the regions of $1600\text{--}1200\text{ cm}^{-1}$ and $4000\text{--}2800\text{ cm}^{-1}$ can be readily associated to its lignocellulosic composition (Gastaldi et al., 1998). An analysis of the structural formula of the methylene blue and of its FTIR spectrum (Fig. 1(a)) shows that there are a number of active centers in the molecule (e.g., dimethylamino groups, nitrogen and sulfur heteroatoms and the π system of the heterocycle) that may participate in interactions with the diversity of functionalities at the press-cake surface. The dimethylamino groups at the edges of the molecule present absorption bands at $2900\text{--}2800\text{ cm}^{-1}$ that can be attributed to the vibrations of the methyl groups in $-\text{N}(\text{CH}_3)_2$ and they are one of the groups that most likely will interact with the adsorbent surface (Ovchinnikov et al., 2007). The bands at $1600\text{--}1400\text{ cm}^{-1}$ and $900\text{--}700\text{ cm}^{-1}$ can be respectively attributed to the vibrations of C–C cycle stretching and aromatic skeletal groups (Liu et al., 2010). Bands at $800\text{--}600\text{ cm}^{-1}$ can be attributed to the vibrations of the C–S–C group at the heterocycle and a band at the $3450\text{--}3400\text{ cm}^{-1}$ can be interpreted as due to a hydrogen bonding of the type O–H...S in the hydrate crystal (Ovchinnikov et al., 2007). In the spectrum for the methylene blue-loaded adsorbent, the most noticeable changes regarding the spectra for the pure adsorbent and for the pure solid dye are those in the $1740\text{--}1500\text{ cm}^{-1}$ region.

Special attention should be paid to the significant increase in the bands at 1658 and 1737 cm^{-1} which are representative of amide ($-\text{CO}-\text{NH}-$) bond formation (Saeed et al., 2009), thus, indicating a methylene blue adsorption of the end-on type. This interaction is also corroborated by the disappearance of the band at 1710 cm^{-1} due to stretching vibrations of $-\text{C}=\text{O}$ in free carboxyl groups (Liu et al., 2010) and the appearance of a small shoulder at 1610 cm^{-1} due to deformation vibrations of $-\text{NH}$ in amide groups. The low-frequency shift of the band at 1550 cm^{-1} in the spectrum for the press-cake to the band at 1519 cm^{-1} characterizes the incorporation of the methylene blue molecule onto the adsorbent surface, as this latter absorption band is due to $-\text{C}=\text{C}-$ stretching vibration mode of aromatic rings in both press-cake and dye molecules conjugated with the stretching vibration mode of $-\text{C}=\text{N}-$ group of the dye molecule.

Enhancement of the absorption band at 895 cm^{-1} from the press-cake spectrum to that of the loaded adsorbent is also an indicative of the enhancement of the aromaticity at the sorbent surface, thus corroborating the analysis of incorporation of the methylene blue molecule onto the surface of the press-cake adsorbent. The effects of π – π type of interactions could not be verified in the methylene blue-loaded adsorbent spectrum presented in Fig. 1.

3.3. Influence of particle size, initial solution pH and adsorbent dosage

Results on the effect of particle size on the adsorption process are displayed in Fig. 2(a). It can be observed that MB uptake increased with the decrease in particle size from 1.00 mm down to 0.43 mm , due to the corresponding increase in surface area, as reported in previous MB adsorption studies (Karagöz et al., 2008; Nunes et al., 2009). However, the fraction that presented smaller diameter ($D < 0.43\text{ mm}$) did not present satisfactory performance. Such unexpected behavior is attributed to the corresponding decrease in particle density associated with grinding, given that the finer particles were suspended in the aqueous MB solution, thus hindering mixing and proper contact between the adsorbent and the adsorbate.

Materials of biological origin are usually quite heterogeneous in their physical constitution and are comprised of distinct parts with distinct densities. The parts where densities are the lowest tend to generate the finest particles upon grinding, in other words, the finest particles generated during grinding of materials of biological origin are produced from the breaking down of the parts with the lowest densities. Also, the finest particles are more significantly affected by other forces present in the suspension, such as surface tension, which tend to enhance their buoyancy in the medium. These results also indicate that the dye molecules are probably adsorbed at the solid outer surface. Based on the results presented in Fig. 2(a), the remaining experiments were conducted employing crambe press cake ground up to the following particle diameter range: $0.43\text{ mm} < D < 0.84\text{ mm}$.

The aqueous solution pH has been reported to present a significant influence on the adsorptive uptake of dyes due to its impact on both the surface binding-sites of the adsorbent and the ionization process of the dye molecule (Oliveira et al., 2008). In the present study, the effect of pH was investigated for values between 5 and 10 and the results are displayed in Fig. 2(b). The increase in sorption capacity comparing results at pH's 5 and 7 is attributed to the fact that, above the pH_{PZC} value (~ 5.7), the adsorbent surface became predominantly negatively charged, enhancing the electrostatic attraction between the surface and MB cations. However, adsorption efficiency decreased with increasing the pH value from 7 to 10. This can be due to MB dimerization and/or reaction with NaOH at high pH values (Nunes et al., 2009). Also, at higher pH ranges hydrophobic interactions between MB molecules in the solution tend to increase and thus hinder the hydrophobic interactions between MB molecules and the adsorbate surface (e.g., π – π type) which are deemed one of the possible mechanisms of adsorption in our study. Based on these results, the remaining tests were conducted at $\text{pH} = 7$, in order to guarantee a negatively charged surface.

It is noteworthy to mention that the pH of the MB solution was measured after all sorption tests, and pH values varied during sorption towards the pH_{PZC} value. Such behavior was attributed to the increase in the number of negative charges at the surface in lieu of the pH of the solution being higher than the pH_{PZC} and, as adsorption takes place, these negative charges are being counterbalanced by the MB cation being adsorbed (e.g., end-on type through formation of amide bonds), thus, restoring the charge balance to a value close to the original pH_{PZC} . The influence of adsorbent dosage on the efficiency of MB removal can be viewed in Fig. 3. Dye removal efficiency increased with the increase in adsorbent dosage. After 6 h, the percent removal of MB varied

from 81 to 91% as the adsorbent concentration was increased from 5 to 30 g L⁻¹. This can be explained by the increase in surface area that results from the increase in adsorbent mass, and the consequent increase in the number of available adsorption sites.

However, the amount of dye adsorbed per unit mass of adsorbent (adsorption capacity) decreased as the adsorbent mass was increased, given the reduction adsorbate/adsorbent ratio. Similar behavior on the effect of adsorbent concentrations on MB adsorption capacity has been discussed in the literature for other types of adsorbents (Oliveira et al., 2008; Uddin et al., 2009a). Given the results shown in Fig. 3, the remaining experiments were conducted with an adsorbent dosage of 10 g L⁻¹.

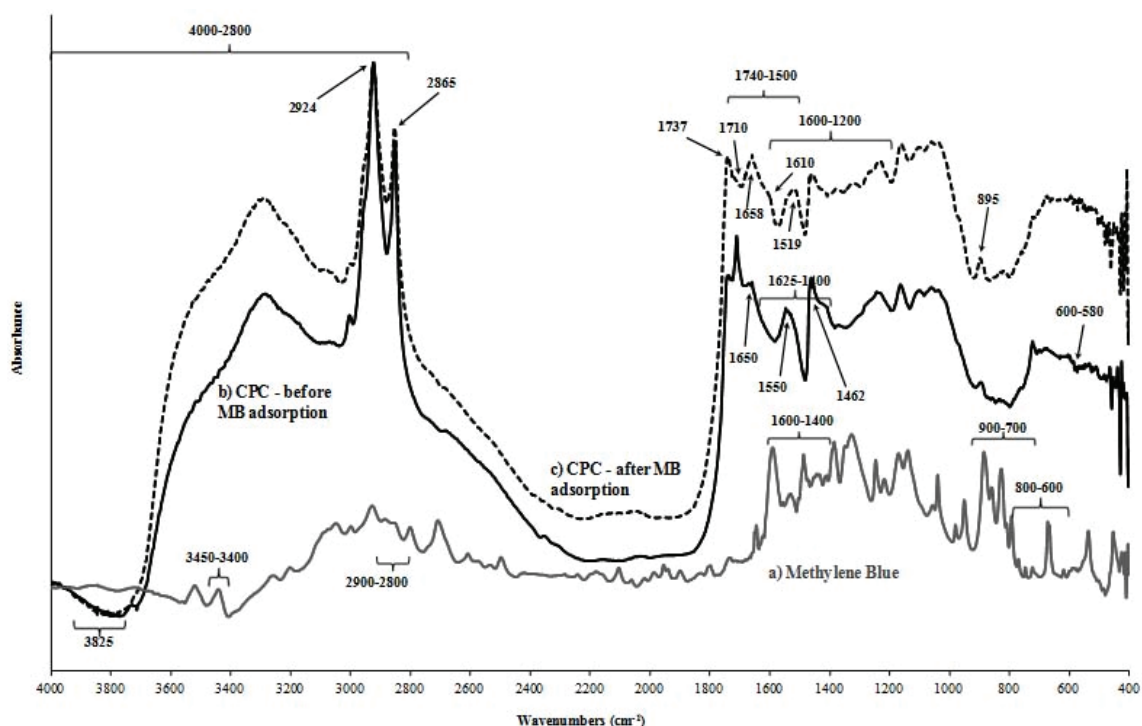


Fig. 1. FTIR spectra of (a) methylene blue (grey), (b) crambe press cake (black) and (c) methylene blue-loaded sorbent (dashed)

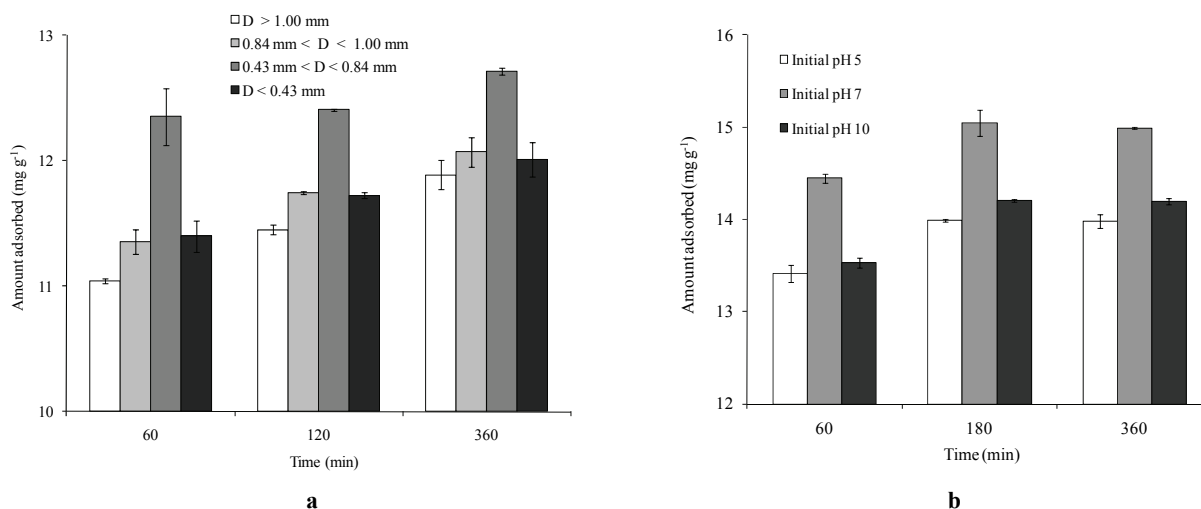


Fig. 2. Effect of (a) particle diameter, D and (b) initial solution pH on MB adsorption by CPC

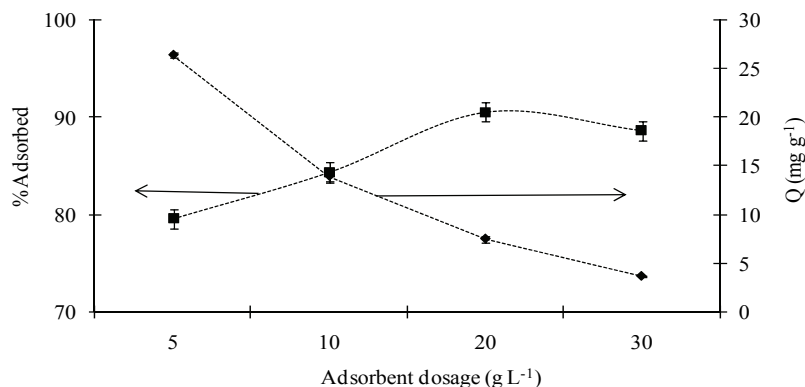


Fig. 3. Effect adsorbent dosage (■ % adsorbed; ◆ amount adsorbed per unit mass - mg g⁻¹) on MB adsorption by CPC

3.4. Adsorption kinetics

The adsorption results shown in Fig. 4 indicate that a contact time of 2 hours is enough to ensure attainment of equilibrium conditions for all the tested values of initial MB concentration. The results presented in Fig. 4 also indicate that MB adsorption by CPC will be significantly affected by the initial MB concentration. An increase in the initial dye concentration led to an increase in the adsorption capacity. The amount of MB adsorbed increased from 3.7 to 51.7 mg g⁻¹ as the initial concentration was raised from 50 to 700 mg L⁻¹. This effect can be attributed to the corresponding increase in driving force (concentration gradient) as the initial initial MB concentration increases (Oliveira et al., 2008).

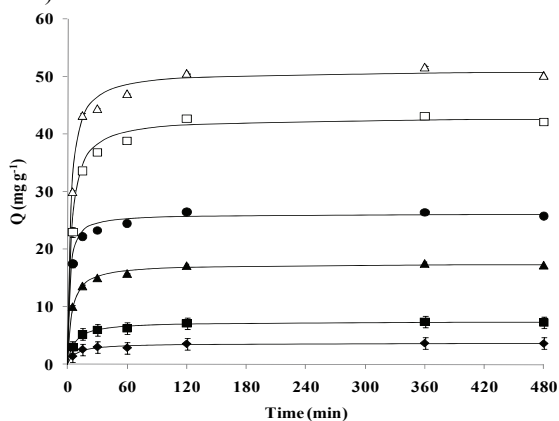


Fig. 4. Effect of contact time on MB adsorption by CPC at 30°C (initial pH 7, dosage 10 g L⁻¹). Initial MB concentration: ◆ 50 mg L⁻¹, ■ 100 mg L⁻¹, ▲ 200 mg L⁻¹, ● 300 mg L⁻¹, □ 500 mg L⁻¹, Δ 700 mg L⁻¹. Solid lines correspond to pseudo-second order kinetics model fits

The controlling mechanism of MB adsorption kinetics was investigated by evaluating pseudo first and second-order models (Ho and McKay, 1998), that can be represented by the following generalized Eq. 1:

$$\frac{dq_t}{dt} = k_n (q_e - q_t)^n \quad (1)$$

where q_e and q_t represent the amount of dye adsorbed per unit mass of adsorbent (mg/g) at equilibrium and at time t , respectively; and k_n is the rate constant for nth order adsorption (k_n units are min⁻¹ and g mg⁻¹ min⁻¹, for n=1 and n=2, respectively). The corresponding equations obtained after integration are (Eqs. 2-3):

Pseudo-first order model or Lagergren (n=1):

$$q_t = q_e (1 - e^{-k_1 t}) \quad (2)$$

Pseudo-second order model (n=2):

$$\frac{t}{q_t} = \frac{1}{k_2 q_e^2} + \frac{t}{q_e} \quad (3)$$

The results obtained for the kinetic parameters are shown in Table 1. Selection of the best model was based on highest R² values coupled with the lowest difference between model estimated and experimental q_e values. Results displayed on Table 1 indicate that MB adsorption by crambe press cake can be satisfactorily described by the pseudo second-order model, indicating chemisorption as the rate-controlling mechanism (Ho and McKay, 1998; Tan et al., 2007). The better fit of the pseudo second order model has been also reported for other types of agricultural wastes and biosorbents employed for MB removal (Ho and McKay, 1998).

Dependence of the adsorption rate constants (k_2) on temperature can provide information about the activation energy of adsorption. Physical adsorption is usually fast and easily reversible, and energy requirements are small (usually below 4.2 kJ mol⁻¹), given that the attraction forces between adsorbate and adsorbent are weak. Chemical adsorption, on the other hand, is specific and involves much stronger forces, and the activation energy presents the same magnitude as the heat of chemical reactions (between 8.4 and 83.7 kJ mol⁻¹) (Aksu et al., 2008). The kinetics rate constant can be expressed as a function of temperature by the following Arrhenius-type relationship (Eq. 4):

$$k_2 = A_0 \exp(-E_A / RT) \quad (4)$$

Table 1. Kinetic parameters for MB adsorption by *Crambe* press cake

MB initial concentration (mg L ⁻¹)	q_e (exp.)*	Pseudo first-order			Pseudo second-order		
		q_e	k_1	R^2	q_e	k_2	R^2
30°C							
50	3.71±0.02	3.46	0.085	0.7612	3.74	0.031	0.9992
100	7.40±0.01	7.00	0.082	0.8626	7.45	0.018	0.9997
200	17.52±0.00	16.77	0.010	0.8640	17.51	0.013	0.9998
300	26.42±0.09	25.52	0.126	0.7916	26.18	0.019	0.9996
500	43.10±0.10	41.37	0.102	0.8547	42.92	0.006	0.9996
700	51.64±0.09	49.18	0.130	0.7265	51.02	0.007	0.9996
40°C							
50	4.01±0.07	3.68	0.152	0.4817	4.09	0.032	0.9989
100	6.67±0.53	6.52	0.149	0.7191	6.73	0.073	0.9997
200	16.08±0.39	15.92	0.110	0.9757	16.21	0.027	0.9999
300	24.23±0.16	23.77	0.197	0.5554	24.39	0.031	0.9998
500	39.99±0.32	39.05	0.161	0.7173	40.32	0.013	0.9999
700	49.28±0.08	48.07	0.217	0.4157	49.51	0.013	0.9998
50°C							
50	3.71±0.04	3.52	0.109	0.7915	3.77	0.032	0.9999
100	8.27±0.04	7.96	0.125	0.7933	8.37	0.032	0.9999
200	17.00±0.24	16.73	0.191	0.7789	17.07	0.044	0.9999
300	25.46±0.09	25.34	0.162	0.9553	25.58	0.052	1.0000
500	40.90±0.32	40.32	0.209	0.5191	41.15	0.026	0.9998
700	48.59±0.49	48.06	0.234	0.5224	48.78	0.032	0.9999

*Average value ± standard deviation

where A_0 corresponds to the frequency factor of sorption and E_A is the activation energy of sorption. The activation energy of MB adsorption by *crambe* press cake was found to increase from 20 to 62 kJ mol⁻¹ as the initial concentration increased, based on the slopes of the corresponding ln k_2 versus 1/ T plots ($R^2 > 0.98$) in the temperature range studied. Such result confirms chemical adsorption.

3.5. Adsorption equilibrium

The adsorption isotherms obtained for experiments performed at 30, 40 and 50°C are displayed in Fig. 5. The shapes of the curves are characteristic of favorable adsorption, given that the adsorption capacity increases with the increase in initial dye concentration. Such behavior was observed in all curves, regardless of the experiment temperature. Information on the tested models and corresponding parameters (obtained by non-linear regression based on least squares minimization, $p < 0.05$) is displayed on Table 2.

Selection of the best fit models was based on highest values of R^2 coupled with the lowest difference between calculated and experimental results. This difference was evaluated according to the following root mean square error measure (Eq. 5):

$$RMS = \sqrt{\sum [(q_{e,est} - q_{e,exp}) / q_{e,exp}]^2 / N} \quad (5)$$

where $q_{e,exp}$ and $q_{e,est}$ correspond to experimental and calculated equilibrium adsorbent amounts, respectively; a N represents the number of experimental isotherm points. MB adsorption from

aqueous solutions by *crambe* press cake was better described by the Freundlich model. This was expected, given the heterogeneous surface of the adsorbent and the fact that it was not submitted to any thermal or chemical treatment that could increase porosity. Previous studies have also shown MB adsorption being better described by Freundlich in comparison to Langmuir. Examples include adsorbents based on coffee grounds (Hirata et al., 2002), on fruit shells and stones (Aygün et al., 2003), and obtained by oven carbonization of defective coffee press cake (Nunes et al., 2009). Evaluation of the applicability of Langmuir model indicates correlation coefficients slightly lower to those obtained by Freundlich and higher RMS values. Temkin model, based on a uniform distribution of binding energies over the adsorbent, also did not provide a satisfactory fit to the experimental data. Such behavior corroborates the non-homogeneous nature of the adsorbent. The Dubinin–Radushkevich (D-R) model did not present a satisfactory fit. Considering that this model is commonly associated to adsorption onto microporous solids (Dubinin et al., 1947) these results indicate that surface adsorption might be the prevailing mechanism in this study.

Maximum monolayer MB uptake capacity (based on Langmuir model) was 79.7 mg g⁻¹. This value is comparable to those of other residue-based adsorbents reported in the literature for MB adsorption at ambient temperature, as can be seen in Table 3. Adsorption capacity was even higher in comparison to some adsorbents that were obtained by thermal and/or chemical treatment of similar types of residues, i.e. seed press cakes. Such results confirm that this type of residue presents an excellent potential as an adsorbent for removal of cationic dyes

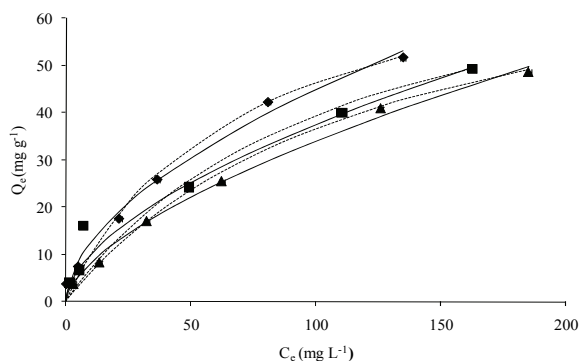


Fig. 5. Adsorption isotherms of MB by CPC (♦ 30°C, ■ 40°C, ▲ 50°C, initial pH 7, dosage 10 g L⁻¹). Solid and dashed lines correspond to Freundlich and Langmuir model fits, respectively

3.6. Thermodynamics parameters

The free energy change (ΔG°), enthalpy change (ΔH°), and entropy change (ΔS°) were determined in order to evaluate the effect of temperature on MB adsorption by CPC. The Gibbs free energy was evaluated as (Eq. 6):

$$\Delta G^\circ = -RT \ln K^\circ \tag{6}$$

where ΔG° is the standard Gibbs free energy change (J), R is the universal gas constant (8.314 J mol⁻¹ K⁻¹), T is the absolute temperature (K)

and K° is the standard thermodynamic apparent equilibrium constant of the adsorption system.

The apparent equilibrium constant is defined as (Eq. 7):

$$K = \frac{C_{ad,e}}{C_e} \tag{7}$$

where C_e and $C_{ad,e}$ correspond to the equilibrium concentration of MB on the solution and on the adsorbent, respectively. K° is obtained as the intercept of the a straight line of the plot of K vs. C_e at different initial concentrations of dye (Aksu et al., 2008). Enthalpy (ΔH°) and entropy (ΔS°) values were obtained from the slope and intercept of a van't Hoff Eq. 8:

$$\ln K^\circ = \frac{\Delta S^\circ}{R} - \frac{\Delta H^\circ}{T} \tag{8}$$

Results for thermodynamic parameters are displayed in Table 4. The negative ΔG° values obtained for MB adsorption at various temperatures confirm the spontaneous characteristic of the process. The negative value of ΔH° confirms the exothermic nature of MB adsorption by crambe press cake and the negative ΔS° value confirms the decreased randomness at the solid-solute interface during biosorption.

Table 2. Adsorption isotherm models and fitting parameters

Model	Equation	Parameter values			R ²			RMS		
		30°C	40°C	50°C	30°C	40°C	50°C	30°C	40°C	50°C
Langmuir	$q_e = \frac{q_0 K_L C_e}{1 + K_L C_e}$	$K_L = 0.014$ $q_0 = 79.7$	$K_L = 0.009$ $q_0 = 83.0$	$K_L = 0.08$ $q_0 = 82.5$	0.9895	0.9876	0.9963	0.1685	0.1765	0.0849
Freundlich	$q_e = K_F C_e^{1/n}$	$K_F = 3.453$ $1/n = 0.557$	$K_F = 2.611$ $1/n = 0.578$	$K_F = 1.929$ $1/n = 0.623$	0.9909	0.9991	0.9960	0.1170	0.0442	0.0299
Temkin	$q_e = (RT/b) \ln(K_T C_e)$	$K_T = 2.318$ $b = 386.50$	$K_T = 0.064$ $b = 277.03$	$K_T = 0.483$ $b = 229.21$	0.7280	0.9084	0.8871	0.4672	0.2781	0.3312
D-R	$q_e = q_0 \exp(-Be^2)$ $e = RT \ln(1 + 1/C_e)$ $E = 1/\sqrt{2B}$	$E = 71.45$ $q_0 = 48.89$	$E = 41.12$ $q_0 = 50.20$	$E = 48.15$ $q_0 = 45.66$	0.9232	0.7974	0.8944	0.2423	0.2834	0.2412

q_e (mg g⁻¹) is the equilibrium adsorption capacity; C_e (mg L⁻¹) is the solute concentration in the aqueous solution, after equilibrium; q_0 (mg g⁻¹) is the maximum adsorption capacity; R is the universal gas constant (8.314 J mol⁻¹ K⁻¹); T (K) is the absolute temperature; E (J/mol²) is the mean free energy; the remaining constants are empirical parameters associated to each specific model.

Table 3. Langmuir based maximum adsorption capacity of several residue-based adsorbents for MB removal at room temperature (25-30°C)

Residue	q _{max} (mg g ⁻¹)	Reference
Almond, walnut and hazelnut shells ^c	1.4 – 8.8	Aygun et al. (2003)
Defective coffee beans press cake – oven activated ^b	14.9	Nunes et al. (2009)
Sunflower oil cake ^c	16.4	Karagöz et al. (2008)
Raphanus Sativus press cake-- oven activated ^b	19.8	Lázaro et al. (2008)
Raphanus Sativus press cake-- microwave activated ^b	29.9	Nunes et al. (2011)
Madhuca indica seeds ^a	40.0	Gottipati and Mishra (2010)
Defective coffee beans press cake –microwave activated ^b	68.5	Franca et al. (2010)
Crambe press cake ^a	79.7	This study
Garlic peel ^a	82.6	Hameed and Ahmad (2009)
Tea waste ^a	85.2	Uddin et al. (2009a)
Coffee husks ^a	90.1	Oliveira et al. (2008)

^ano activation; ^bthermal activation only; ^cthermal/chemical activation;

Table 4. Thermodynamic parameters for MB adsorption by Crambe press cake

Parameter	Temperature (°C)		
	30	40	50
K^o	93.40	22.18	8.42
ΔG^o (KJ mol ⁻¹)	-11.4	-8.1	-5.7
ΔH^o (KJ mol ⁻¹)		-11.8	
ΔS^o (J mol ⁻¹ K ⁻¹)		-0.29	

3.7. Continuous studies

The effects of varying solution inlet concentrations and flow rates on the continuous MB removal on a fixed bed of crambe press cake are shown in the breakthrough curves depicted in Fig. 6(a) and 6(b), respectively.

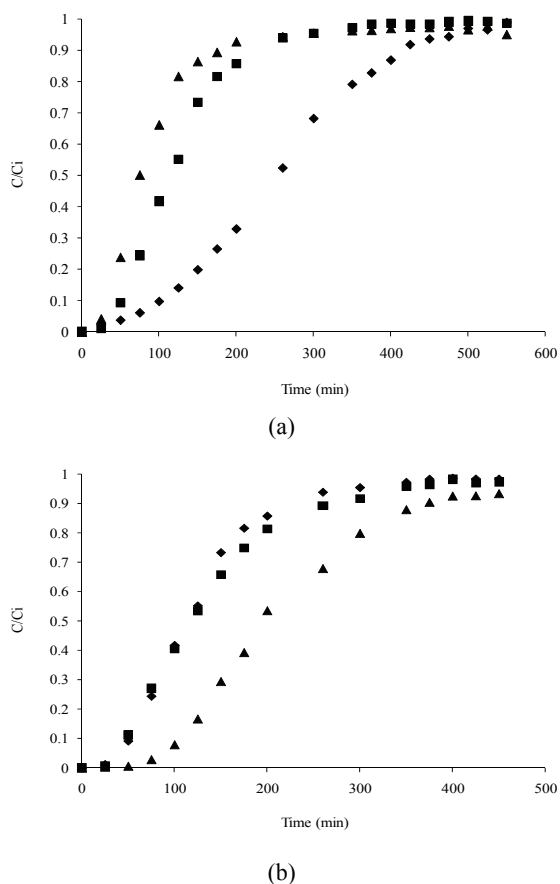


Fig. 6. Experimental breakthrough curves for different values of (a) inlet flow concentration (◆ 200 mg L⁻¹, ■ 500 mg L⁻¹, ▲ 700 mg L⁻¹; flow rate = 21.5 mL min⁻¹; pH = 5.8) and (b) flow rate (◆ 21.5 mL min⁻¹, ■ 18.5 mL min⁻¹, ▲ 11.5 mL min⁻¹; inlet concentration = 500 mg L⁻¹; pH = 5.8)

It can be noticed from Fig. 6(a) and 6(b) that the breakthrough curves present the ideal “S” shape profile that is characteristic of adsorbates of small molecular sizes and also of adsorbents that present relatively small sized particles (Florido et al., 2010).

From Fig. 6(a), it can be seen that the increase in the MB inlet concentration resulted on a

shortening of both the breakthrough time and the bed service time, indicating that the adsorbent was more quickly saturated (Goyal et al., 2009; Han et al., 2009). The increase in MB inlet concentration also caused a steepening of the slope of the breakthrough curve (i.e., a shortening of the mass transfer zone), thus reducing the volume treated before saturation. A decrease in the MB inlet concentration caused the breakthrough times to become longer and the breakthrough curves became more dispersed (a larger mass transfer zone). This is attributed to a lower concentration gradient causing slower transport due to a smaller intra-particle diffusion coefficient (Han et al., 2009; Florido et al., 2010).

The effects observed on the breakthrough curves when the flow rate was increased (Fig. 6(b)) were a decrease in both the volume treated and the breakthrough time, i.e., breakthrough occurred faster. Accordingly, at when flow rates were decreased, longer breakthrough times and service times were observed (Xu et al., 2009). The breakthrough curve became steeper when the flow rate was increased. This indicates that the mass transfer zone was shortened, implying on higher intra-particle diffusion effects as previously reported in other fixed bed adsorption studies (Uddin et al., 2009b). As the flow rate increases the boundary layer around the particles becomes thinner, thus reducing external (film) mass transfer resistance. Nonetheless, Goyal and co-workers (2009) showed that, if the flow rate is increased beyond a certain value, the rate of adsorption will decrease because the residence time of the adsorbate in the column is diminished (there is not enough time for the diffusional mass transfer to occur). Even though the flow rate in this study was not increased beyond such value, it can be clearly seen from Fig. 6(b) that increasing the flow rate above 21.5 mL/min will probably not improve adsorption performance, given that there were no significant differences between the breakthrough curves obtained for 18.5 and 21.5 mL/min.

Bohart-Adams, Yoon-Nelson and Dose-Response models were evaluated for description of the breakthrough curves. Details on model equations, estimated model parameters and the adsorption capacity (obtained by nonlinear regression) are presented in Table 5 together with the respective experimentally determined values. The corresponding adjusted curves are shown in Fig. 7.

The classic Bohart-Adams model (Bohart and Adams, 1920) is based on the assumption that the adsorption rate is proportional to both the residual capacity of the solid and the concentration of the adsorbing species. Although it has been repeatedly stated in the literature that the Bohart-Adams model is fit to describe only the initial part of the breakthrough curve (Calero et al., 2009; Han et al., 2009), in this work, this model was reasonably fitted only to the ascending portion of breakthrough experimental data (Fig. 7). Discrepancies in the fitting can be observed both in the initial and in the

tailing portion of the breakthrough curve. The discrepancies in the tailing portion are usually attributed to the phenomena of axial dispersion, which is not taken into account in the model, and which becomes more pronounced as the concentration gradient between the adsorbate solution and the adsorbent decreases throughout the column, i.e., as the saturation of the adsorbent is approached. As seen from the data presented in Table 5, the rate constant (k_{BA}) estimated from the nonlinear fitting of Bohart-Adams model does not vary significantly with variations in both flow rate and adsorbate inlet concentration, which means that the rate controlling mechanism is actually the adsorption kinetics rather than the mass transfer or the intraparticle diffusion. This was confirmed by an exact match of the parameters obtained for both the Bohart-Adams and the Thomas model fitting to the breakthrough data (not shown here for reasons of avoiding redundancy), considering that Thomas model was developed under the assumption that adsorption kinetics is the controlling mechanism (Chu, 2010).

Considering that the Bohart-Adams model presented a reasonable fit to the entire range of the ascending portion of the breakthrough experimental data and that the rate constant is representative of the adsorption mechanism throughout the entire length of the bed, the only plausible explanation for the discrepancy observed at the initial portion of the curve may be that the dominant MB adsorption mechanism in this portion is one with a faster kinetics than that imbued in the model, the later being the one actually occurring in the ascending portion of the curve. Recall that MB can be adsorbed by either interactions of the end-on type or interactions of the π - π type (Franca et al., 2010) and, also, different adsorption mechanisms have been proposed, depending on the characteristics of the adsorbent and of the MB solution (Ofomaja, 2008).

Further, according to the equilibrium and thermodynamic data obtained in the batch tests (best fit of Freundlich model and $-20 < \Delta G^\circ < 0$ KJ mol⁻¹), the possibility of multilayer adsorption should be considered (Han et al., 2010).

The model proposed by Yoon and Nelson (1994) is based on the premise that the probability of adsorption of molecule decreases at a rate that is proportional to both the adsorption and breakthrough probabilities.

Yoon-Nelson model presented correlation coefficients similar to those of Bohart-Adams model. This was somewhat expected, since the mathematical forms of the equations are the same. The Dose-Response model was the one that provided the best description of the experimental data. This model was proposed for the description of heavy metal biosorption in columns (Yan et al., 2001). It is has been recently employed in other studies and it is also commonly used to describe different processes in pharmacology. However, the nature of the model inhibits any analysis of the mechanism involved in the adsorption throughout the column.

The results obtained in the present study for experimental adsorption capacity are presented in Table 6 in comparison to capacity values reported from other works in which MB was adsorbed in different low-cost adsorbents. The adsorption capacity for the MB-CPC system in a fixed bed adsorption process can be considered significant when compared to other capacity data for other MB-adsorbent systems.

4. Conclusions

Experiments were conducted to investigate the potential of *Crambe abyssinica* press cake, a residue from crambe oil and/or biodiesel production, as and adsorbent.

Table 5. Bohart-Adams, Yoon-Nelson and Dose-Response model parameters at different adsorbate solution inlet concentrations and flow rates

Model	Equation	Parameters	C_i (mg L ⁻¹) [$Q = 21.5$ mL min ⁻¹]			Q (mL min ⁻¹) [$C_i = 500$ mg L ⁻¹]		
			200	500	700	11.5	18.5	21.5
Bohart-Adams	$\frac{C}{C_i} = \frac{\exp(K_{BA}C_i t)}{\exp(K_{BA}C_i t) + \exp(K_{BA}N_o z / U_o) - 1}$ $q_0 = N_o z S / m$	$K_{BA} \times 10^5$ (L mg ⁻¹ min ⁻¹)	6.952	5.515	4.774	3.317	4.553	5.515
		q_0 (mg g ⁻¹)	90.5	105.7	104.5	101.2	97.2	105.7
		R^2	0.9993	0.9955	0.9865	0.9924	0.9923	0.9955
Yoon-Nelson	$\frac{C}{C_i} = \frac{I}{I + \exp[k_{YN}(t_{50} - t)]}$ $q_0 = \frac{C_i Q t_{50}}{1000m}$	K_{YN} (min ⁻¹)	0.0139	0.0276	0.0334	0.0167	0.0221	0.0276
		q_0 (mg g ⁻¹)	89.7	104.5	102.2	100.3	95.1	104.5
		t_{50} (min)	253.1	117.9	82.4	211.6	124.7	117.9
R^2	0.9993	0.9955	0.9865	0.9955	0.9955	0.9955		
Dose-Response	$\frac{C}{C_i} = I - \frac{I}{I + (C_i V_{ef} / q_0 m)^v}$	a (-)	3.3387	3.0611	2.5978	3.3495	2.5737	3.0611
		q_0 (mg g ⁻¹)	84.1	98.5	94.4	94.1	88.0	98.5
		R^2	0.9960	0.9993	0.9982	0.9993	0.9994	0.9993
Experimental		q_0 (mg g ⁻¹)	83.1	102.5	108.3	96.7	96.5	102.5
		t_{50} (min)	252.9	115.5	75.0	194.0	118.6	115.5

C (mg L⁻¹) represents the adsorbate (MB) concentration in the fluid at the outlet or at any point in the column; C_i (mg L⁻¹) is the adsorbate concentration in the fluid at the inlet of the column; N_o (mg L⁻¹) is the sorption capacity per unit volume of fixed bed, z (cm) represents the bed depth; U_o (cm min⁻¹) corresponds to the superficial velocity; S (cm²) is the bed cross section area; t_{50} represents the time required for 50% breakthrough; Q (mL min⁻¹) is the volumetric flow rate through the column; m (g) is the adsorbent mass; and V_{ef} (mL) is the volume of the effluent (mL); all the remaining constants correspond to empirical parameters associated to each specific model

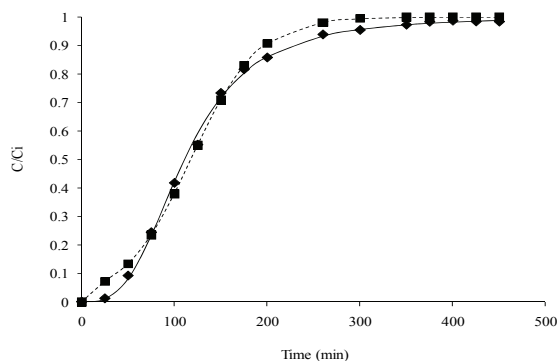


Fig. 7. The experimental (◆) and predicted breakthrough curves using — — Bohart–Adams, ■ Yoon and Nelson, and —●— Dose–Response models for the adsorption of MB by crambe press cake at an inlet MB concentration of 500 mg/L

Table 6. Experimental fixed-bed adsorption capacities ($q_{0,exp}$) for MB removal by low-cost adsorbents

Adsorbent	C_0 (mg L ⁻¹)	Bed height (cm)	$q_{0,exp}$ (mg/g)	Reference
Peach stones activated carbon	200	0.2	71.3	Attia et al. (2008)
Crambe press-cake	500	6.0	83.1-108.3	This study
Phoenix tree leaf powder	100	15.0	152.0	Han et al. (2009)
Jackfruit leaf powder	300	5.0	260.0	Uddin et al. (2009b)

Equilibrium data demonstrated favorable adsorption. FTIR spectra indicated the formation of amide bonds between carboxylic groups at sorbent surface and the dimethylamino groups at the edges of the methylene blue molecules to be one of the main mechanisms of adsorption.

The process was found to be chemical adsorption, given the high value of activation energy. Fixed-bed breakthrough curves presented the “S” profile characteristic of adsorbates of small molecular sizes and also of adsorbents comprised of relatively small sized particles.

The maximum value of uptake capacity for this system was higher in comparison to adsorbents obtained by thermal and/or chemical treatment of other seed press cakes, confirming the adsorption potential of the material.

Acknowledgements

The authors acknowledge financial support from the following Brazilian Government Agencies: CNPq and FAPEMIG.

References

Ajmal M., Rao R.A.K., Khan M.A., (2005), Adsorption of copper from aqueous solution on *Brassica cumpestris* (mustard oil cake), *Journal of Hazardous Materials*, **122**, 177–183.
 Aksu Z., Tatli A.I., Tunc O., (2008), A comparative adsorption/biosorption study of Acid Blue 161: Effect

of temperature on equilibrium and kinetic parameters, *Chemical Engineering Journal*, **42**, 23-39.
 Ali, I., Asim, M., Khan, T.A., (2012) Low cost adsorbents for the removal of organic pollutants from wastewater, *Journal of Environmental Management*, **113**, 170-183.
 Aygun A., Yenisoay-Karakas S., Duman I., (2003), Production of granular activated carbon from fruit stones and nutshells and evaluation of their physical, chemical and adsorption properties, *Microporous and Mesoporous Materials*, **66**, 189-195.
 Bhatnagar A., Sillanpää M., (2010), Utilization of agro-industrial and municipal waste materials as potential adsorbents for water treatment - A review, *Chemical Engineering Journal*, **157**, 277-296.
 Boehm H.P., (1994), Some aspects of the surface chemistry of carbon blacks on other carbons, *Carbon*, **32**, 759-769.
 Bohart G.S., Adams E.Q., (1920), Some aspects of the behavior of charcoal with respect to chlorine, *Journal of the American Chemical Society*, **42**, 523–544.
 Boucher J., Steiner Z., Marison I.W., (2007), Bio-sorption of atrazine in the press cake from oil seeds, *Water Research*, **41**, 3209–3216.
 Bulgariu L., Cojocaru C., Robu B., Macoveanu M., (2007), Equilibrium isotherms studies for sorption of lead ions from aqueous solutions using Romanian peat sorbent, *Environmental Engineering and Management Journal*, **6**, 425-430.
 Calero M., Hernainz F., Blazquez G., Tenorio G., Martin-Lara M.A., (2009), Study of Cr (III) biosorption in a fixed-bed column, *Journal of Hazardous Materials*, **171**, 886-893.
 Chu K.H., (2010), Fixed bed sorption: Setting the record straight on the Bohart-Adams and Thomas models, *Journal of Hazardous Materials*, **177**, 1006–1012.
 Dubinin M.M., Zaverina E.D., Radushkevich L.V., (1947), Sorption and structure of active carbons. I. Adsorption of organic vapors, *Russian Journal of Physical Chemistry*, **21**, 1351–1362.
 Falasca S.L., Flores N., Lamas M.C., Carballo S.M., Anschau A., (2010), *Crambe abyssinica*: An almost unknown crop with a promissory future to produce biodiesel in Argentina, *International Journal of Hydrogen Energy*, **35**, 5808-5812.
 Florido A., Valderrama C., Arevalo J.A., Casas I., Martinez M., Miralles N., (2010), Application of two sites non-equilibrium sorption model for the removal of Cu(II) onto grape stalk wastes in a fixed-bed column, *Chemical Engineering Science*, **156**, 298-304.
 Franca A.S., Oliveira L.S., Nunes A.A., Alves C.C.O., (2010), Microwave assisted thermal treatment of defective coffee beans press cake for the production of adsorbents, *Bioresource Technology*, **101**, 1068-1074.
 Garg U., Kaur M.P., Garg V.K., Sud D., (2007), Removal of hexavalent chromium from aqueous solution by agricultural waste biomass, *Journal of Hazardous Materials*, **140**, 60–68.
 Garg U., Kaur M.P., Jawa G.K., Sud D., Garg V.K., (2008), Removal of cadmium(II) from aqueous solutions by adsorption on agricultural waste biomass, *Journal of Hazardous Materials*, **154**, 1149–1157.
 Gastaldi G., Capretti G., Focher B., Cosentino C., (1998), Characterization and proprieties of cellulose isolated from the *Crambe abyssinica* hull, *Industrial Crops and Products*, **8**, 205–218.
 Gottipati R., Mishra S., (2010), Application of biowaste (waste generated in biodiesel plant) as an adsorbent for the removal of hazardous dye - methylene blue -

- from aqueous phase, *Brazilian Journal of Chemical Engineering*, **27**, 357-367.
- Goyal M., Bhagat M., Dhawan R., (2009), Removal of mercury from water by fixed bed activated carbon columns, *Journal of Hazardous Materials*, **171**, 1009–1015.
- Guerrero-Coronilla I., Morales-Barrera L., Villegas-Garrido T.L., Cristiani-Urbina E., (2014), Biosorption of Amaranth dye from aqueous solution by roots, leaves, stems and the whole plant of *E. crassipes*, *Environmental Engineering and Management Journal*, **13**, 1917-1926.
- Hameed B.H., Ahmad A.A., (2009), Batch adsorption of methylene blue from aqueous solution by garlic peel, an agricultural waste biomass, *Journal of Hazardous Materials*, **164**, 870-875.
- Han R., Wang Y., Zhao X., Wang Y., Xie F., Cheng J., Tang M., (2009), Adsorption of methylene blue by phoenix tree leaf powder in a fixed-bed column: experiments and prediction of breakthrough curves, *Desalination*, **245**, 284-297.
- Han R., Zhang L., Song C., Zhang M., Zhu H., Zhang L., (2010), Characterization of modified wheat straw, kinetic and equilibrium study about copper ion and methylene blue adsorption in batch mode, *Carbohydrate Polymers*, **79**, 1140–1149.
- Hirata M., Kawasaki N., Nakamura T., Matsumoto K., Kabayama M., Tamura T., Tanada S., (2002), Adsorption of dyes onto carbonaceous materials produced from coffee grounds by microwave treatment, *Journal of Colloid and Interface Science*, **254**, 17-22.
- Ho Y.S., McKay G., (1998), Comparison of chemisorption kinetic models applied to pollutant removal on various sorbents, *Process Safety and Environmental Protection*, **76**, 332-340.
- Karagöz S., Tay T., Ucar S. Erdem M., (2008), Activated carbons from waste biomass by sulfuric acid activation and their use on methylene blue adsorption, *Bioresource Technology*, **99**, 6214–6222.
- Lázaro D.A., Mansur M.B., Franca A.S., Oliveira L.S., Rocha S.D.F., (2008), Performance of cold-pressed cake from *Raphanus sativus* (L. Var.) oilseeds, a solid residue from biodiesel production, as adsorbent for basic dyes, *International Journal of Chemical Engineering*, **1**, 147-160.
- Liu Y., Zheng Y., Wang A., (2010), Enhanced adsorption of Methylene Blue from aqueous solution by chitosan-g-poly (acrylic acid)/vermiculite hydrogel composites, *Journal of Environmental Sciences*, **22**, 486–493.
- Lopez-Núñez P.V., Aranda-García E., Cristiani-Urbina M.C., Morales-Barrera L., Cristiani-Urbina E., (2014) Removal of hexavalent and total chromium from aqueous solutions by plum (*P. domestica* L.) tree bark, *Environmental Engineering and Management Journal*, **13**, 1927-1938.
- Noh J.S., Schwarz J.A., (1990), Effect of HNO₃ treatment on the surface acidity of activated carbons, *Carbon*, **28** 675-682.
- Nunes A.A., Franca A.S., Oliveira L.S., (2009), Activated carbons from waste biomass: an alternative use for biodiesel production solid residues, *Bioresource Technology*, **100**, 1786-1792.
- Nunes D.L., Franca A.S., Oliveira L.S., (2011), Use of *Raphanus sativus* L. press cake, a biodiesel processing solid residue, in the production of adsorbents by microwave activation, *Environmental Technology*, **32**, 1073-1083.
- Ofomaja E.A., (2008), Sorptive removal of Methylene blue from aqueous solution using palm kernel fibre: Effect of fibre dose, *Biochemical Engineering Journal*, **40**, 8-18.
- Oliveira L.S., Franca A.S., Alves T.M., Rocha S.D.F., (2008), Evaluation of untreated coffee husks as potential biosorbents for treatment of dye contaminated waters, *Journal of Hazardous Materials*, **155**, 507-512.
- Ovchinnikov O.V., Chernykh S.V., Smirnov M.S., Alpatova D.V., Vorob'eva R.P., Latyshev A.N., Evlev A.B., Utekhin A.N., Lukin A.N., (2007), Analysis of interaction between the organic dye methylene blue and the surface of AgCl(I) microcrystals, *Journal of Applied Spectroscopy*, **74**, 809-816.
- Saeed A., Iqbal M., Zafar S.I., (2009), Immobilization of *Trichoderma viride* for enhanced methylene blue biosorption: Batch and column studies, *Journal of Hazardous Materials*, **168**, 406–415.
- Tan I.A.W., Hameed B.H., Ahmad A.L., (2007), Equilibrium and kinetic studies on basic dye adsorption by oil palm fibre activated carbon, *Chemical Engineering Journal*, **127**, 111–119.
- Uddin M.T., Islam M.A., Mahmud S., Rukanuzzaman M., (2009a), Adsorptive removal of methylene blue by tea waste, *Journal of Hazardous Materials*, **164**, 53-60.
- Uddin M.T., Rukanuzzaman M., Rahman Khan M.M., Islam M.A., (2009b), Adsorption of methylene blue from aqueous solution by jackfruit (*Artocarpus heterophyllus*) leaf powder: A fixed-bed column study, *Journal of Environmental Management*, **90**, 3443-3450.
- Wang Y.P., Tang J.S., Chu C.Q., Tian J., (2000), A preliminary study on the introduction and cultivation of *Crambe abyssinica* in China, an oil plant for industrial uses, *Industrial Crops and Products*, **12**, 47-52.
- Xu X., Gao B., Wang W., Yue Q., Wang Y., Ni S., (2009), Adsorption of phosphate from aqueous solutions onto modified wheat residue: Characteristics, kinetic and column studies, *Colloids and Surfaces B: Biointerfaces*, **70**, 46–52.
- Yan G.Y., Viraraghavan T., Chem M., (2001), A new model for heavy metal removal in a biosorption column, *Adsorption Science & Technology*, **19**, 25–43.
- Yoon Y.H., Nelson J.H., (1984), Application of gas adsorption kinetics I. A theoretical model for respirator cartridge service life, *American Industrial Hygiene Association Journal*, **45**, 509–516.